

# Optical Thermophoresis for Quantifying the Buffer Dependence of Aptamer Binding\*\*

Philipp Baaske,\* Christoph J. Wienken, Philipp Reineck, Stefan Duhr, and Dieter Braun

Quantification of biomolecular binding reactions in their native environment is crucial for biology and medicine. However, reliable methods are rare. We have developed a new immobilization-free method in which thermophoresis, the movement of molecules in a thermal gradient, is used to determine binding curves; this method can be used to study binding in various buffers as well as in human blood serum. The assay does not rely on surface contact and requires only an unspecific fluorescence marker on one of the binding partners.

Aptamers are nucleic acid ligands selected *in vitro* for their ability to bind to specific molecular targets.<sup>[1–4]</sup> They are promising candidates for diagnostic applications because of their affinity and specificity—comparable to that of antibodies—and the ease with which novel aptamers can be designed.<sup>[5]</sup> Aptamers have been implemented in a variety of sensing technologies<sup>[6]</sup> including optical approaches like “aptamer beacons”,<sup>[7]</sup> electronic-sensing strategies,<sup>[8]</sup> and techniques based on changes in mass<sup>[9]</sup> or force.<sup>[10]</sup>

In most aptamer-based binding assays, the signal transduction mechanism depends on the molecular recognition mechanism. As a result the aptamers must be designed not only to adopt an appropriate conformation to bind to a target (recognition) but also to undergo a binding-induced conformational change, which affects the fluorescence of a dye<sup>[8]</sup> or the electron transfer<sup>[9]</sup> of a redox tag to an electrode (signal transduction). This linkage between target recognition and signal transduction sets obstacles for the design of aptamers. Often aptamers must be modified with two labels, which results in reduced binding affinity or even complete suppression of binding.<sup>[11]</sup> These restrictions can be reduced by separating the molecular recognition from the signal transduction by using additional competitor oligonucleotides, complementary to the aptamer, as signal transduction elements.<sup>[12]</sup>

Herein we describe a novel approach for the quantification of aptamer–target interactions which separate molecular recognition from signal transduction and require an aptamer with only one unspecific tag. In this way binding can be probed under physiological conditions, under diffusion in complex biological fluids.

The approach is based on the directed movement of molecules along temperature gradients, an effect termed thermophoresis.<sup>[13–16]</sup> A temperature difference in space  $\Delta T$  leads to a depletion of the solvated biomolecule in the region of elevated temperature, quantified by the Soret coefficient  $S_T$  [Eq. (1)].

$$c_{\text{hot}}/c_{\text{cold}} = \exp(-S_T \Delta T) \quad (1)$$

Thermophoresis depends on the interface between molecule and solvent. Under constant buffer conditions, thermophoresis depends on the size, charge, and solvation entropy of the molecules<sup>[15,16]</sup> and is not dependent on the concentration of the probed molecule unless millimolar concentrations are reached.<sup>[17,18]</sup> The thermophoresis of an aptamer *A* typically differs significantly from that of an aptamer–target complex *AT* because of changes in size, charge, or solvation energy. We used this difference in the molecule’s thermophoresis to quantify the binding of a 5.6 kDa aptamer to the protein thrombin (37 kDa) as well as the binding of a 8.3 kDa aptamer to AMP (0.3 kDa) and ATP (0.6 kDa) in titration experiments under constant buffer conditions. We found that binding affinities depend on the buffer conditions and that the binding constants determined in 10 % and 50 % serum differ significantly from those measured in buffer solution.

The thermophoretic movement of the fluorescently end-labeled aptamer is measured by monitoring the fluorescence distribution *F* inside a glass capillary, which contains 500 nL of sample, with an epifluorescence microscope (Figure 1 a). The microscopic temperature gradient is generated by an IR laser (1480 nm); the light is focused into the capillary and strongly absorbed by water.<sup>[15,16,19]</sup> The temperature of the aqueous solution in the laser spot is raised by  $\Delta T = 8$  K. Before the IR laser is switched on, a homogeneous fluorescence distribution  $F_{\text{cold}}$  is measured inside the capillary (Figure 1 b). When the IR laser is switched on, two effects, on different timescales, contribute to the new fluorescence distribution  $F_{\text{hot}}$ . The thermal relaxation time is fast (roughly 50 ms) and induces a drop in fluorescence of the dye owing to its intrinsic temperature dependence. On the slower timescale of diffusion (roughly 10 s), the aptamers move from the locally heated region to the outer cold regions.<sup>[16,20]</sup> The local concentration of aptamers decrease in the heated region until it reaches a steady-state distribution (Figure 1 b).

[\*] P. Baaske, C. J. Wienken, P. Reineck, Prof. D. Braun  
Ludwig-Maximilians-Universität München  
Systems Biophysics, Department of Physics  
Center for NanoScience (CeNS), 80799 Munich, (Germany)

P. Baaske, S. Duhr  
NanoTemper Technologies GmbH  
Amalienstrasse 54, 80799 Munich (Germany)  
Fax: (+49) 89-21801-6558  
E-mail: philipp.baaske@nanotemper.de  
Homepage: <http://www.nanotemper.de>

[\*\*] We thank the LMU Innovative Initiative Functional NanoSystem (FUNS) and the Excellence Cluster NanoSystems Initiative Munich (NIM) for financial support.

Supporting information for this article is available on the WWW under <http://dx.doi.org/10.1002/anie.200903998>.

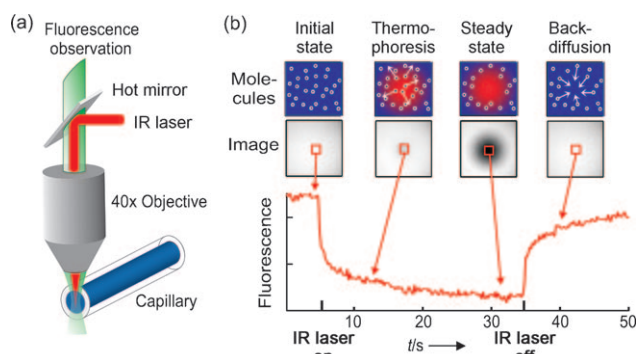


**Figure 1.** Thermophoresis assay. a) The blood serum inside the capillary is locally heated with a focused IR laser, which is coupled into an epifluorescence microscope using a heat-reflecting “hot” mirror. b) The fluorescence inside the capillary is imaged with a CCD camera, and the normalized fluorescence in the heated spot is plotted against time. The IR laser is switched on at  $t=5$  s, the fluorescence decreases as the temperature increases, and the labeled aptamers move away from the heated spot because of thermophoresis. When the IR laser is switched off, the molecules diffuse back.

While the molecular diffusion  $D$  dictates the kinetics of depletion, the Soret coefficient  $S_T$  describes the concentration ratio under steady-state conditions  $c_{\text{hot}}/c_{\text{cold}} = \exp(-S_T \Delta T) \approx 1 - S_T \Delta T$  for a temperature increase  $\Delta T$ .<sup>[15,16]</sup> The normalized fluorescence  $F_{\text{norm}} = F_{\text{hot}}/F_{\text{cold}}$  measures mainly this concentration ratio, in addition to the temperature dependence of the dye fluorescence  $\partial F/\partial T$ . In the linear approximation we find:  $F_{\text{norm}} = 1 + (\partial F/\partial T - S_T) \Delta T$ .<sup>[16]</sup> Because of the linearity of the fluorescence intensity and the thermophoretic depletion, the normalized fluorescence from the unbound aptamer  $F_{\text{norm}}(\text{A})$  and the bound complex  $F_{\text{norm}}(\text{AT})$  superpose linearly. If  $x$  is used to denote the fraction of aptamers bound to targets, the changing fluorescence signal during the titration of target  $T$  can be given by Equation (2).

$$F_{\text{norm}} = (1-x) F_{\text{norm}}(\text{A}) + x F_{\text{norm}}(\text{AT}) \quad (2)$$

Based on the capacitor model of thermophoresis,<sup>[15,21]</sup> confirmed for thin Debye layers in experiments using polystyrene beads,<sup>[15]</sup> double-stranded DNA,<sup>[15]</sup> single-stranded DNA,<sup>[16]</sup> and Ludox silica particles,<sup>[22]</sup> we can discuss the change in  $S_T$  expected from changes in charge  $Q_{\text{eff}}$  or hydrodynamic radius  $R$  upon binding. Assuming negligible offsets from non-ionic contributions, we find  $S_T \propto (Q_{\text{eff}}/R)^2$ . Under linear approximation,  $S_T$  changes by  $\Delta S_T/S_T = 2(\Delta Q_{\text{eff}}/Q_{\text{eff}} - \Delta R/R)$ . Only for the unlikely case that  $Q_{\text{eff}}$  is directly proportional to  $R$  would no change in  $S_T$  be expected. However, neglected contributions from solvation entropy<sup>[15]</sup> could contribute to binding even under these conditions.

We measured the thermophoresis of 100 nm thrombin aptamer labeled at the 5' end with the fluorophore Cy5<sup>[23]</sup> in 10% human serum (Figure 2). The concentration of thrombin ranges from 0 nM to 19 500 nM. The low concentrations ensure that the serum and buffer do not change upon addition of thrombin and keep the thermophoresis of the aptamer constant. The observed time traces of the pure aptamer differ significantly from the traces of aptamers bound to

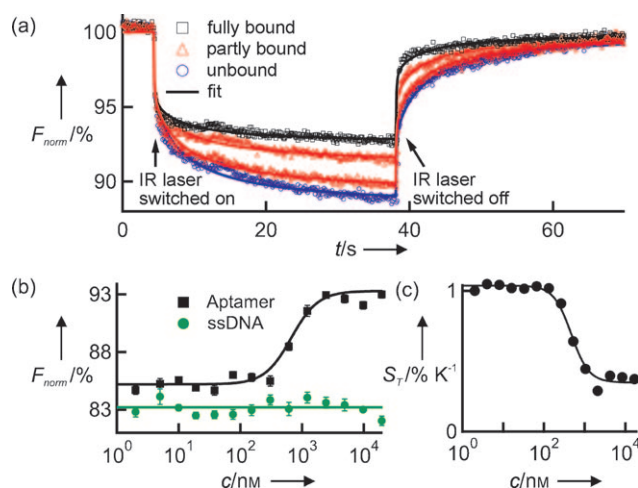


**Figure 2.** Aptamer–thrombin binding in 10% human serum. a) The thermophoretic depletion of unbound aptamer is about twice that of aptamers bound to thrombin. b) The normalized fluorescence  $F_{\text{norm}}$  at  $t=30$  s is plotted for different concentrations of thrombin (black). The thermophoresis of random 25-mer ssDNA (green) shows no dependence on thrombin concentration. c) The Soret coefficient  $S_T$  also reflects the binding;  $S_T$  was determined based on an analytical model of thermophoresis.<sup>[16]</sup>

thrombin (Figure 2a). Plotting the normalized fluorescence  $F_{\text{norm}}$  at a given time  $t$  against the thrombin concentration results in a binding curve (Figure 2b) with an  $EC_{50}$  value of  $680 \pm 80$  nM and a Hill coefficient of 2. Control experiments with a randomly chosen sequence of ssDNA show no thrombin-dependent changes in either the thermophoretic signal (Figure 2b) or the absolute fluorescence, in either 10% or 50% serum. This indicates that neither interactions of thrombin with the Cy5 label, nor unspecific interactions of thrombin with ssDNA are present.

As detailed previously,<sup>[16]</sup> we used a two-dimensional finite element simulation to infer from the time traces the Soret coefficient  $S_T$ , the diffusion coefficient  $D$ , and the temperature dependence of the fluorescence  $\partial F/\partial T$ . The binding of the aptamer to thrombin mostly leads to a change in  $S_T$ , which decreases from  $1.05 \text{ K}^{-1}$  to  $0.35 \text{ K}^{-1}$  (Figure 2c). Owing to their linear relationship,  $F_{\text{norm}}$  and the  $S_T$  both report the binding (Figure 2b,c). Neither the temperature-dependent fluorescence change  $\partial F/\partial T$  nor the diffusion coefficient  $D$  changed during the titration. Notably the determination of  $D$  is likely to be hampered by fitting crosstalk with  $\partial F/\partial T$ .

The thermophoretic perturbation creates a direct fluorescence ratio signal  $F_{\text{norm}}$  that reveals changes in the observed molecule that stem from changes in size, charge, or solvation entropy of the molecule. It does not rely on the notoriously difficult task of observing binding-induced size changes by measuring small changes in the diffusion coefficient  $D$  as, for example, in fluorescence correlation spectroscopy (FCS). As shown in Figure 3a, the approach can be used in buffers and equally well in complex biological liquids like blood serum without significantly loss of sensitivity or specificity as is the case with surface-based technologies such as surface plasmon resonance (SPR).

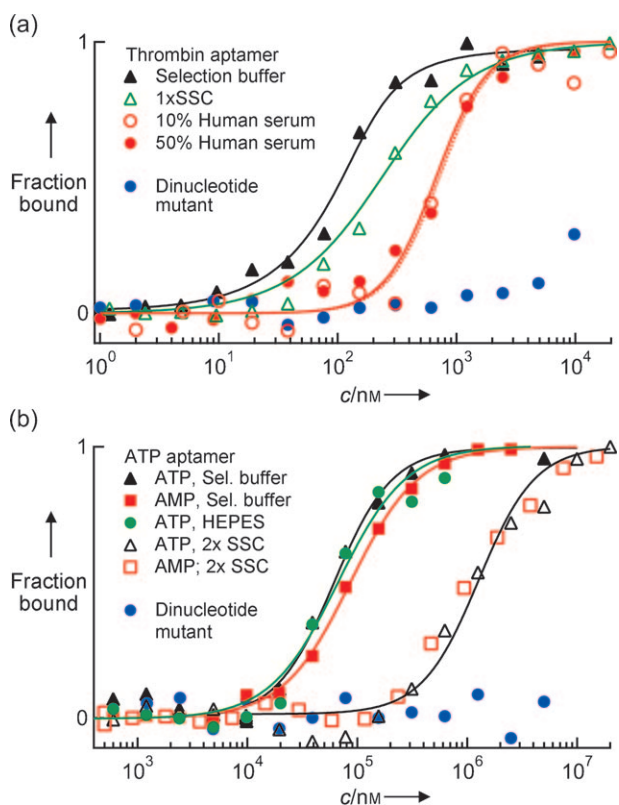


**Figure 3.** Binding curves in various buffers. a) Aptamer–thrombin binding in selection buffer, 1 × SSC (sodium citrate) and in 10% and 50% untreated human serum. b) Aptamer binding to ATP and AMP in selection buffer, HEPES, and 2 × SSC. The fraction of bound aptamers is derived according to Equation (2).

To further show the broad applicability of the thermophoretic quantification of binding, we also measured the binding of an aptamer to ATP and AMP<sup>[24]</sup> (Figure 3b) in different buffers. In all cases, binding was reported with a high signal-to-noise ratio (SNR), even in 50% human serum. For example, SNR = 93 was found for the binding of an aptamer to 0.3 kDa AMP in selection buffer, and SNR = 23 was found for the binding to thrombin in 50% human serum (see the Supporting Information). As control oligonucleotides we used DNA sequences that differed from the respective aptamer sequences in only two nucleotide mutations (Figure 3a,b “Dinucleotide mutant”).

The dissociation constant  $K_D = 30 \pm 19$  nM obtained for the aptamer–thrombin binding (Figure 3a) in selection buffer is in good agreement with the reported  $K_D = 25 \pm 25$  nM<sup>[23]</sup> measured in the same buffer. However, Buff et al.<sup>[25]</sup> also reported slightly reduced binding affinity resulting from 5'-extensions of the thrombin–aptamer. In SSC buffer the dissociation constant increases to  $K_D = 190 \pm 20$  nM and in 50% (10%) human serum the binding was best fitted with the Hill equation, yielding  $EC_{50} = 720 \pm 100$  nM ( $670 \pm 80$  nM) and a cooperativity of  $n = 2$ .

The aptamer–ATP/AMP binding (Figure 3b) shows the cooperative binding of more than one ATP or AMP per aptamer, which is consistent with literature reports.<sup>[7,26]</sup> In the selection buffer, the  $EC_{50}$  values for ATP ( $EC_{50} = 60 \pm 4$  μM)

and AMP ( $EC_{50} = 87 \pm 5$  μM) agree well with the reported values.<sup>[7,12]</sup> Measurements of the ATP binding in HEPES buffer ( $EC_{50} = 67 \pm 8$  μM) confirm these results. In all cases the Hill coefficient was  $n = 1.4$ . Interestingly, in 2 × SSC buffer, the  $EC_{50}$  values of the ATP/AMP–aptamer binding were both strongly shifted to lower affinities, resulting in  $EC_{50} = 1100 \pm 100$  μM. Note that the ATP solutions were cooled to prevent hydrolysis of ATP.

As stated by Cho and Ellington,<sup>[6]</sup> the aptamer–target binding depends strongly on the chosen buffer: The binding of the aptamers in the respective selection buffers always showed the highest affinity (Figure 3). For aptamer–thrombin binding in human serum, the shift to lower affinities ( $EC_{50} = 720$  nM) and enhanced cooperativity ( $n = 1.5$ ) may be because of interactions of the thrombin with components of the blood serum. For ATP–aptamer binding the unexpected significant shift to lower affinities in the SSC buffer is likely an effect of a competing interaction of the strongly negative citrate<sup>3-</sup> ion of the SSC buffer with the Mg<sup>2+</sup> ions, as the latter are essential for aptamer–ATP/AMP binding.

In conclusion, we have developed a purely optical analytical method based on the thermophoresis of solvated molecules for the study of aptamer–target interactions in bulk solution. The sample volume is very low: 500 nL of which only 2 nL is probed. The signal transduction of binding is separated from the molecular recognition, which provides more freedom in the design of aptamers. The assay is robust and simple as no secondary reactions for detection are required. The dynamic range of the thermophoresis binding assay extends from nM to mM target concentrations, and the binding to low-mass targets such as AMP can also be quantified. The measurement can be performed in complex liquids such as blood and in simple standard buffers equally well. As a result, the approach will enable the determination of the affinity of aptamer-based drug candidates, for example spiegelmers,<sup>[27]</sup> in biological liquids under close to physiological conditions. The method is also applicable for screening new aptamers since the binding of unlabeled aptamers to a labeled target can also be quantified by thermophoresis.

### Experimental Section

For imaging, we used a Zeiss Axiotech Vario microscope with a 40x Plan Fluor oil objective, numerical aperture 1.3. The fluorescence was excited with a red high-power LED Luxeon III (LXHL-LD3C). Fluorescence filters for Cy5 (F36–523) were purchased from AHF-Analysentechnik (Tübingen, Germany). Detection was provided with the Sencam EM CCD camera from PCO AG (Kelheim, Germany). Fused-silica capillaries from Polymicro Technologies (Phoenix, USA) with an inner diameter of 100 μm and a volume of about 500 nL were used for the measurements.

The temperature gradients were created with an IR laser diode (Furukawa FOL1405-RTV-617-1480,  $\lambda = 1480$  nm,  $\kappa = 320$  μm for water, 320 mW maximum power) purchased from AMS Technologies AG (Munich, Germany). The IR laser beam was coupled into the path of fluorescence light with a heat-reflecting “hot” mirror (NT46-386) from Edmund Optics (Barrington, USA) and is focused into the fluid with the microscope objective. The temperature inside the capillary was measured by the known temperature-dependent fluorescence of the TAMRA dye.<sup>[19]</sup> The temperature in the solution

was increased by 8 K in the beam center with a  $1/e^2$  diameter of 25  $\mu\text{m}$ . All measurements were performed at room temperature.

The changes in fluorescence were analyzed in a region around the center of heating with a diameter of about 50  $\mu\text{m}$ . The images were corrected for background and bleaching of the fluorescence.<sup>[16,20]</sup>

The human  $\alpha$ -thrombin was purchased from Haematologic Technologies Inc. (Essex Junction, USA; specific activity 3593  $\text{U mg}^{-1}$ ; MW = 36.7 kDa). Human serum, AMP, and ATP were purchased from Sigma Aldrich (Munich, Germany).

The labeled DNA oligonucleotides were synthesized by Metabion (Martinsried, Germany). The sequences of the oligonucleotides, with mutations as small letters, are: Thrombin aptamer: 5'-Cy5-TGGTTGGTGTGGTTGGT-3'; thrombin dinucleotide mutant: 5'-Cy5-TGGTTGtTGTGGTtGT-3'; ATP aptamer: 5'-Cy5-CCTGGGGGAGTATTGCGGAGGAAGG-3'; ATP aptamer dinucleotide mutant: 5'-Cy5-CCTtGGGGAGTATTGCGGAtGAAGG-3'; ssDNA: 5'-Cy5-TAGTTCTAATGTGTATCTCAATTTT-3'.

Measurements were conducted in the following buffers: Thrombin-aptamer: Selection buffer:<sup>[23]</sup> 20 mM Tris-HCl pH 7.4, 150 mM NaCl, 5 mM KCl, 1 mM  $\text{CaCl}_2$ , 1 mM  $\text{MgCl}_2$ , 0.01% TWEEN20, 4% BSA. For the human serum measurements this buffer was mixed 1:1 with 100% human serum.  $1 \times \text{SSC}$ : 15 mM sodium citrate, pH 7.4, 150 mM NaCl, 5 mM KCl, 1 mM  $\text{CaCl}_2$ , 1 mM  $\text{MgCl}_2$ , 0.01% TWEEN20, 4% BSA. ATP-aptamer: Selection buffer:<sup>[24]</sup> 20 mM Tris-HCl pH 7.6, 300 mM NaCl, 5 mM  $\text{MgCl}_2$  and 0.01% TWEEN20.  $2 \times \text{SSC}$ : 30 mM sodium citrate, pH 7.4, 300 mM NaCl, 5 mM  $\text{MgCl}_2$ , 0.01% TWEEN20. HEPES: 20 mM HEPES pH 7.5, 300 mM NaCl, 5 mM  $\text{MgCl}_2$ , and 0.01% TWEEN20. For ATP the pH of the buffers was measured for different ATP concentrations with the pH-sensitive dye BCECF (see the Supporting Information).

The aptamer and the mutant concentrations were maintained at 100 nM (thrombin-aptamer) and 500 nM (ATP-aptamer) during all experiments. The aptamers were denatured and renatured prior to the experiments to ensure that they reached their active conformation. The solutions were incubated for 2 h after the oligonucleotides had been mixed with the different target molecules.

The  $K_D$  values for thrombin were obtained by fitting the fraction of bound aptamers to the quadratic solution of the binding reaction equilibrium, derived from the law of mass action, with  $K_D$  as single free parameter.<sup>[11]</sup> The  $\text{EC}_{50}$  values were obtained from fitting the binding curves with the Hill equation (see the Supporting Information).

Received: July 20, 2009

Published online: February 23, 2010

**Keywords:** aptamers · DNA · drug discovery · immobilization-free methods · proteins

- [1] G. Mayer, *Angew. Chem.* **2009**, *121*, 2710–2727; *Angew. Chem. Int. Ed.* **2009**, *48*, 2672–2689.
- [2] A. D. Ellington, J. W. Szostak, *Nature* **1990**, *346*, 818–822.
- [3] C. Tuerk, L. Gold, *Science* **1990**, *249*, 505–510.
- [4] D. L. Robertson, G. F. Joyce, *Nature* **1990**, *344*, 467–468.
- [5] B. Boese, K. Corbino, R. Breaker, *Nucleosides Nucleotides Nucleic Acids* **2008**, *27*, 949–966.
- [6] E. Cho, J. Lee, A. Ellington, *Annu. Rev. Anal. Chem.* **2009**, *2*, 241–264.
- [7] S. Jhaveri, R. Kirby, R. Conrad, E. Maglott, M. Bowser, R. Kennedy, G. Glick, A. Ellington, *J. Am. Chem. Soc.* **2000**, *122*, 2469–2473.
- [8] Y. Xiao, A. A. Lubin, A. J. Heeger, K. W. Plaxco, *Angew. Chem.* **2005**, *117*, 5592–5595; *Angew. Chem. Int. Ed.* **2005**, *44*, 5456–5459.
- [9] S. Song, L. Wang, J. Li, C. Fan, J. Zhao, *TrAC Trends Anal. Chem.* **2008**, *27*, 108–117.
- [10] D. Ho, K. Falter, P. Severin, H. E. Gaub, *Anal. Chem.* **2009**, *81*, 3159–3164.
- [11] S. Beyer, W. Dittmer, F. Simmel, *J. Biomed. Nanotechnol.* **2005**, *1*, 96–101.
- [12] N. Li, C. M. Ho, *J. Am. Chem. Soc.* **2008**, *130*, 2380–2381.
- [13] C. Ludwig, *Sitzungsber. Akad. Wiss. Wien Math.-Naturwiss. Kl.* **1856**, *20*, 539.
- [14] S. Iacopini, R. Piazza, *Europhys. Lett.* **2003**, *63*, 247–253.
- [15] S. Duhr, D. Braun, *Proc. Natl. Acad. Sci. USA* **2006**, *103*, 19678–19682.
- [16] P. Reineck, C. J. Wienken, D. Braun, *Electrophoresis* **2010**, *31*, 279–286.
- [17] J. K. G. Dhont, *J. Chem. Phys.* **2004**, *120*, 1632–1641.
- [18] J. Rauch, W. Köhler, *J. Chem. Phys.* **2003**, *119*, 11977–11988.
- [19] P. Baaske, S. Duhr, D. Braun, *Appl. Phys. Lett.* **2007**, *91*, 133901.
- [20] S. Duhr, S. Arduini, D. Braun, *Eur. Phys. J. E* **2004**, *15*, 277–286.
- [21] J. K. G. Dhont, S. Wiegand, S. Duhr, D. Braun, *Langmuir* **2007**, *23*, 1674–1683.
- [22] H. Ning, J. K. G. Dhont, S. Wiegand, *Langmuir* **2008**, *24*, 2426–2432.
- [23] L. C. Bock, L. C. Griffin, J. A. Latham, E. H. Vermaas, J. J. Toole, *Nature* **1992**, *355*, 564–566.
- [24] D. E. Huizenga, J. W. Szostak, *Biochemistry* **1995**, *34*, 656–665.
- [25] M. C. R. Buff, F. Schäfer, B. Wulffen, J. Müller, B. Pötzsch, A. Heckel, G. Mayer, *Nucleic Acids Res.* **2009**, DOI: 10.1093/nar/gkp1148.
- [26] C. H. Lin, D. J. Patel, *Chem. Biol.* **1997**, *4*, 817–832.
- [27] C. Maasch, K. Buchner, D. Eulberg, S. Vonhoff, S. Klussmann, *Nucleic Acids Symp. Ser.* **2008**, *52*, 61–62.